Journal of Organometallic Chemistry 695 (2010) 1111–1118

Contents lists available at ScienceDirect

Journal of Organometallic Chemistry

journal homepage: www.elsevier.com/locate/jorganchem

Interaction of 2-(2′,6′-dialkylphenylazo)-4-methylphenols with iridium. C–H activation and migration of alkyl group

Suparna Baksi [a], Dipravath Kumar Seth [a], Haregewine Tadesse [b], Alexander J. Blake [b], Samaresh Bhattacharya [a,*]

[a] Department of Chemistry, Inorganic Chemistry Section, Jadavpur University, Kolkata 700 032, India
[b] School of Chemistry, University of Nottingham, University Park, Nottingham NG7 2RD, UK

ARTICLE INFO

Article history:
Received 30 October 2009
Received in revised form 1 January 2010
Accepted 7 January 2010
Available online 20 January 2010

Keywords:
2-(2′,6′-Dialkylphenylazo)-4-methylphenols
Organoiridium complexes
C–H and C–C bond activation

ABSTRACT

Reaction of 2-(2′,6′-diethylphenylazo)-4-methylphenol ($\mathbf{L^2}$) with [Ir(PPh$_3$)$_3$Cl] afforded two organoiridium complexes **3** and **4** via C–H bond activation of an ethyl group in the arylazo fragment of the $\mathbf{L^2}$ ligand. In both the complexes the azo ligand binds to iridium as a dianionic tridentate C,N,O-donor. Two triphenylphosphines and a hydride (in the case of complex **3**) or chloride (in the case of complex **4**) are also coordinated to the metal center. A similar reaction of [Ir(PPh$_3$)$_3$Cl] with 2-(2′,6′-diisopropylphenylazo)-4-methylphenol ($\mathbf{L^3}$) yielded another organoiridium complex **5**, where migration of one *iso*-propyl group from its original location (say, the 2′ position) to the corresponding third position (say, the 4′ position) took place through C–C bond activation. In this complex the modified azo ligand binds to iridium as a dianionic tridentate C,N,O-donor. Two triphenylphosphines and a hydride are also coordinated to the metal center. The structures of complexes **3** and **4** have been optimized through DFT calculations. The structure of complex **5** has been determined by X-ray crystallography. All the complexes show characteristic ^{1}H NMR signals and intense transitions in the visible region. Cyclic voltammetry on all the complexes shows an oxidation within 0.66–1.10 V vs SCE, followed by a second oxidation within 1.15–1.33 V vs SCE and a reduction within −0.96 to −1.07 V vs SCE.

1. Introduction

Metal mediated chemical transformation of organic substrates belongs to an area of research, which has been receiving considerable attention [1–16]. A key step in such reactions is the activation of C–H or C–C bond in the organic substrates, which is usually achieved through their interaction with soft metal centers. The metal–carbon bonded species, so generated, serve as active intermediates towards formation of the final products. Metal promoted C–H and C–C bond activation of organic molecules has thus been of significant current interest [17–35]. We have been active, for quite some time, in the synthesis of organometallic complexes via platinum-group metal mediated C–H bond activation of organic ligands in general [36–53] and of 2-(arylazo)-4-methylphenols (**I**) in particular [44–49], and the present work has emerged from our continued interest in this area. In this study iridium has been selected as the platinum-group metal for promoting

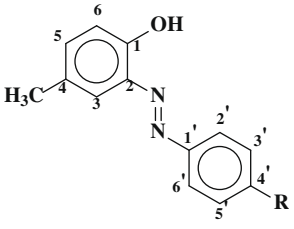

I

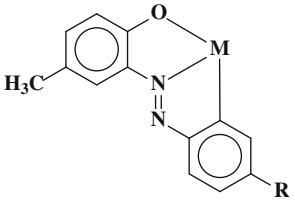

II

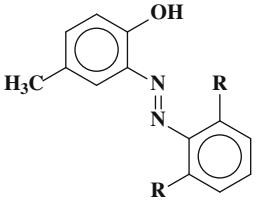

III

R	L
CH_3	L^1
C_2H_5	L^2
$CH(CH_3)_2$	L^3

* Corresponding author.
E-mail address: samaresh_b@hotmail.com (S. Bhattacharya).

0022-328X/$ - see front matter © 2010 Elsevier B.V. All rights reserved.
doi:10.1016/j.jorganchem.2010.01.015

C–H or C–C bond activation and $[Ir(PPh_3)_3Cl]$ has been utilized as the iridium starting material. Upon reaction with $[Ir(PPh_3)_3Cl]$, the 2-(arylazo)-4-methylphenols (**I**) were observed to undergo C–H activation at one *ortho*-position (say, the 2′ position) of the phenyl ring in the arylazo fragment and bind to the metal center as tridentate C,N,O-donors (**II**) affording cyclometalated complexes [46]. This has led us to explore the reactivity of some modified 2-(arylazo)phenols (**III**), in which both the *ortho*-positions of the phenyl ring in the arylazo fragment are strategically blocked by alkyl groups with the intention of inducing metal-mediated C–C bond activation at one of the *ortho*-positions. Initially, reaction of 2-(2′,6′-dimethylphenylazo)-4-methylphenol ($\mathbf{L^1}$) was carried out with $[Ir(PPh_3)_3Cl]$, where one of the two *ortho* methyl groups was found to undergo C–H activation to afford organoiridium complexes (**1** and **2**) [52]. Although an *ortho* methyl group in ligand $\mathbf{L^1}$ was observed to undergo interesting elimination [53], migration [51] and oxidative migration [50], such a metal–carbon bond formation via methyl C–H bond

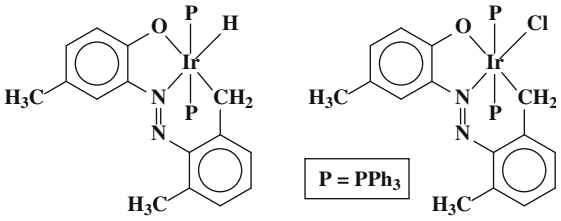

1 **2**

activation of ligand $\mathbf{L^1}$ was not experienced. It is also noteworthy that methyl C–H activation is less common than phenyl C–H activation [54–62]. This interesting reactivity of $\mathbf{L^1}$ has prompted us to scrutinize reactions of two related 2-(2′,6′-dialkylphenylazo)-4-methylphenols ($\mathbf{L^2}$ and $\mathbf{L^3}$) with iridium. The main objective of the present study has been to see whether these two new ligands, which bear larger alkyl groups (ethyl and *iso*-propyl) at the 2′ and 6′ positions, undergo any iridium-mediated C–H or C–C bond activation. Reactions of $\mathbf{L^2}$ and $\mathbf{L^3}$ with $[Ir(PPh_3)_3Cl]$ have been observed to afford interesting organoiridium complexes via C–H (in case of ligand $\mathbf{L^2}$) and C–C (in case of ligand $\mathbf{L^3}$) bond activations. An account of the chemistry of these organoiridium complexes is presented herein, with special reference to their formation, structure and spectral and electrochemical properties.

2. Results and discussion

2.1. Synthesis and characterization

As delineated in the introduction, the main objective of the present study was to see whether ligands similar to $\mathbf{L^1}$ containing alkyl groups at the 2′ and 6′ positions which are larger than a methyl group (*e.g.* ethyl in $\mathbf{L^2}$ and *iso*-propyl in $\mathbf{L^3}$), can undergo similar reaction with $[Ir(PPh_3)_3Cl]$ causing C–H or C–C bond activation of one of the two *ortho* alkyl groups. Reaction of 2-(2′,6′-diethylphenylazo)-4-methylphenol ($\mathbf{L^2}$) with $[Ir(PPh_3)_3Cl]$ in refluxing toluene in the presence of triethylamine was carried out first, which afforded a pink complex **3** and a red complex **4**. Preliminary characterization of complex **3** indicated the presence of two triphenylphosphines, a hydride and a de-protonated $\mathbf{L^2}$ ligand in it. The ^1H NMR spectrum of this complex (*vide infra*) further suggested that the ligand $\mathbf{L^2}$ is coordinated to the metal center as a tridentate C,N,O-donor (**IV**) via loss of one phenolic proton and a proton from one ethyl group of the arylazo

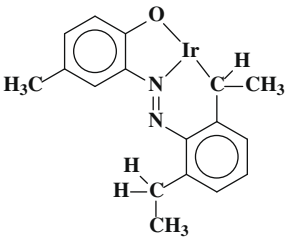

IV

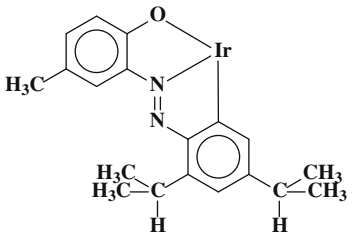

V

fragment. Mass spectral and microanalytical data are found to be in excellent agreement with this composition of complex **3**. Preliminary characterizations on complex **4** show that it is very similar to complex **3** in composition and stereochemistry, the only difference being that a chloride is coordinated to iridium instead of a hydride. Structural characterization of complexes **3** and **4** by X-ray crystallography was not possible since single crystals of these species could not be grown. However, structures of both the complexes were geometrically optimized through DFT calculations [63,64]. The optimized structure of complex **3** is shown in Fig. 1 and some selected bond parameters are given in Table 1. The optimized structure of complex **4** and some selected bond parameters have been deposited as

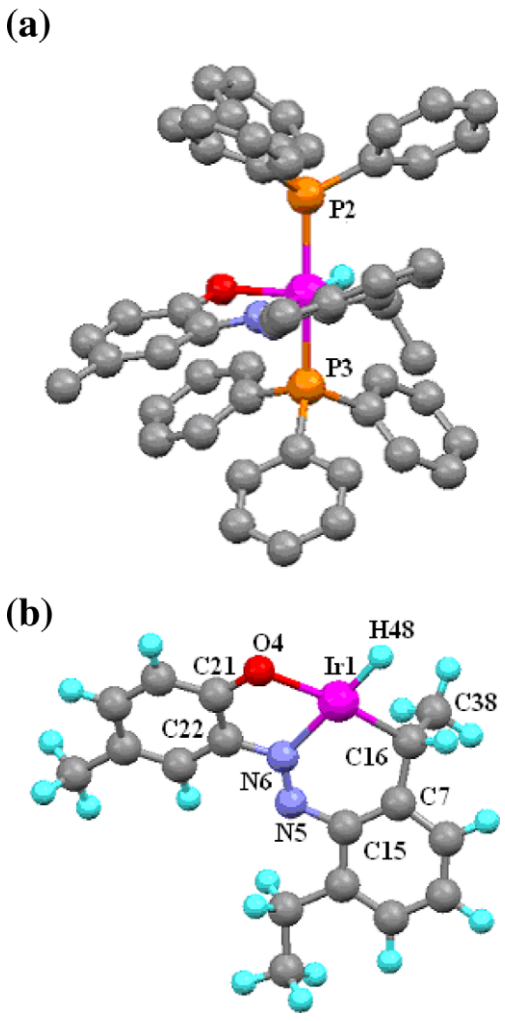

Fig. 1. (a) Optimized structure of complex **3** (phenyl rings of the phosphine ligands have been added replacing hydrogens), and (b) view of the equatorial plane with the axial triphenylphosphine ligands removed for clarity.

Table 1
Selected bond lengths (Å) and bond angles (°) for complex **3**.

Bond lengths (Å)	
Ir(1)–P(2)	2.3707
Ir(1)–P(3)	2.3892
Ir(1)–O(4)	2.2038
Ir(1)–N(6)	2.0795
Ir(1)–C(16)	2.1083
Ir(1)–H(48)	1.6142
N(5)–N(6)	1.2721
O(4)–C(21)	1.3133
Bond angles (°)	
P(3)–Ir(1)–P(2)	167.79
H(48)–Ir(1)–N(6)	178.28
O(4)–Ir(1)–C(16)	173.56
O(4)–Ir(1)–N(6)	79.81
N(6)–Ir(1)–C(16)	92.68

Supplementary material (Fig. S1 and Table S1). The computed bond parameters are found to be comparable with those observed in related complexes for which X-ray crystallographic structure determinations are available [52]. Therefore it can be inferred that, as observed earlier during reaction of $\mathbf{L^1}$ with $[Ir(PPh_3)_3Cl]$ [52], a similar C–H activation of an ethyl group in $\mathbf{L^2}$ took place during formation of complexes **3** and **4**.

Reaction of 2-(2′,6′-diisopropylphenylazo)-4-methylphenol ($\mathbf{L^3}$) with $[Ir(PPh_3)_3Cl]$ was carried out in an analogous manner. However, in contrast to the earlier reaction this afforded a blue complex **5**. Preliminary characterization of complex **5** indicated the presence of two triphenylphosphines, a hydride and a de-protonated $\mathbf{L^3}$ ligand. However, unlike complexes **1**, **2**, **3** and **4**, no indication of C–H activation of any *iso*-propyl group of ligand $\mathbf{L^3}$ during formation of complex **5** was obtained. The ^{1}H NMR spectrum of complex **5** shows clear signals for two *iso*-propyl groups and three singlets (1H each) in the aromatic region at 6.01, 6.38 and 6.66 ppm. As only one singlet could be expected from the *para*-cresol fragment of the azo-ligand, the appearance of three singlets suggested that some unexpected reaction must have taken place in this azo-ligand during formation of complex **5**. To ascertain the stereochemistry of complex **5**, as well as the status of ligand $\mathbf{L^3}$ within it, its structure has been determined by X-ray crystallography. The structure determination reveals (Fig. 2) that an interesting transformation of ligand $\mathbf{L^3}$ has indeed taken place during formation of complex **5**, whereby an *iso*-propyl group has migrated from its original location (say, the 2′ position) and is inserted (via loss of a proton) into the C–H bond at the corresponding 4′ position, thus generating an *iso*-propyl group at the 4′ position, and the modified ligand is bound to iridium as a C,N,O-donor (**V**). Iridium therefore occupies a $HCNOP_2$ coordination sphere, which is significantly distorted from ideal octahedral geometry, as reflected in the bond parameters around the metal center. The coordinated tridentate ligand $\mathbf{L^3}$ and the hydride define the equatorial plane around the iridium center, and the two triphenylphosphines are disposed mutually *trans* in the two axial positions. The Ir–P distances are quite normal and so are the Ir–C, Ir–N, Ir–O, C–O and N–N bond lengths within the C,N,O-chelated fragment (Table 2) [46,52]. The mass spectrum of complex **5**, which shows the $[M-H]^+$ peak at 1011, and the observed microanalytical data are also in excellent agreement with this composition.

The exact mechanisms behind formation of complexes **3**, **4** (via C–H bond activation of ligand $\mathbf{L^2}$) and **5** (via C–C bond activation of $\mathbf{L^3}$), are not completely clear. However, the sequences shown in Schemes 1 and 2 seem probable. During the formation of complexes **3** and **4** (Scheme 1), ligand $\mathbf{L^2}$ initially binds to the metal center in $[Ir(PPh_3)_3Cl]$ via oxidative insertion of iridium into the phenolic O–H bond and a triphenylphosphine gets dissociated simultaneously, producing two geometric isomers (**A**

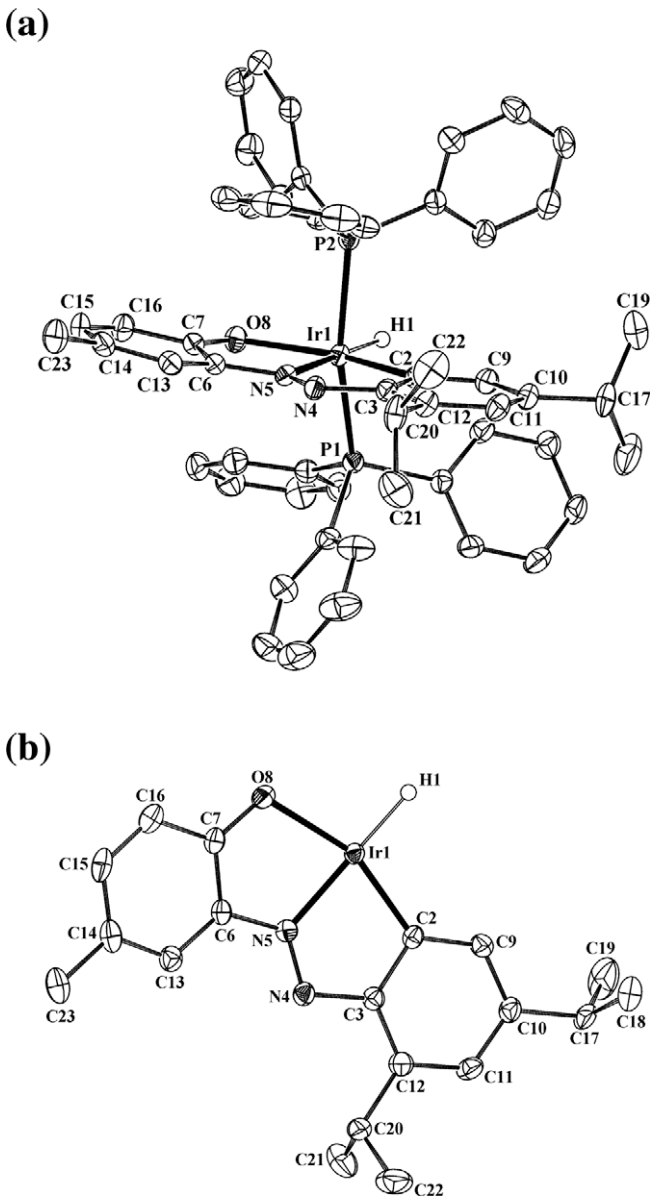

Fig. 2. (a) Crystal structure of complex **5**, and (b) view of the equatorial plane with the axial triphenylphosphine ligands removed for clarity. Except for the coordinated hydride, all hydrogen atoms are omitted for clarity. The hydride H atom could not be located but it is added in a calculated position.

Table 2
Selected bond lengths (Å) and bond angles (°) for complex **5**.

Bond lengths (Å)	
Ir(1)–P(1)	2.3052(9)
Ir(1)–P(2)	2.3066(9)
Ir(1)–O(8)	2.168(2)
Ir(1)–N(5)	2.023(2)
Ir(1)–C(2)	2.039(3)
Ir(1)–H(1)	1.60[a]
N(4)–N(5)	1.281(3)
O(8)–C(7)	1.309(4)
Bond angles (°)	
P(1)–Ir(1)–P(2)	163.16(3)
O(8)–Ir(1)–C(2)	157.44(10)
N(5)–Ir(1)–H(1)	180[a]
N(5)–Ir(1)–C(2)	77.76(11)
O(8)–Ir(1)–N(5)	79.69(9)

[a] Values used to calculate the position of this atom.

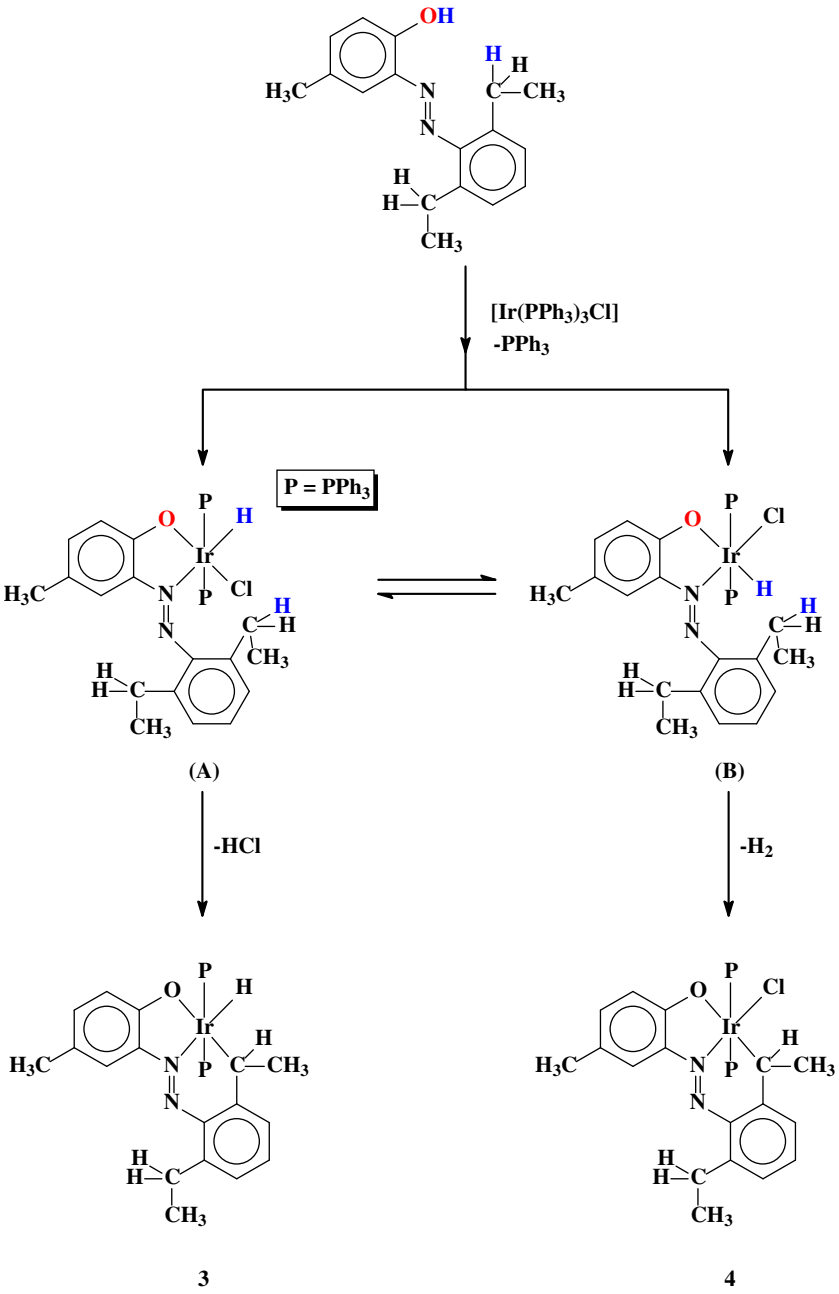

Scheme 1. Proposed scheme for the formation of complexes **3** and **4**.

and **B**) of a hydride intermediate which are believed to remain in equilibrium. In intermediate **A** the coordinated hydride is *cis* to the phenolate oxygen and the coordinated chloride is *trans*, while in the other intermediate **B** the relative disposition of the coordinated hydride and chloride is reversed. Structures of both the intermediates have been geometrically optimized through DFT calculations and the optimized structures along with their respective energies are shown in *Fig.* S2 (Supplementary material). Both the intermediates are found to have comparable energies, which is in accordance with the proposed equilibrium existing between these two species. In the optimized structure of intermediate **A**, the 2′,6′-diethylphenyl fragment is almost orthogonal to the *para*-cresol fragment. In this structure, a methylene hydrogen atom is only 1.527 Å away from the metal-bound chloride subtending a C–H···Cl angle of 105.59°, indicating weak C–H···Cl hydrogen bonding interaction. During the permissible rotation of the 2′,6′-diethylphenyl fragment around the C15–N5 bond and that of the ethyl group around the C7–C16 bond, the methylene C–H bond can come closer to the Ir–Cl bond and would eventually collide with it. This closeness facilitates formation of the iridium–carbon bond in the final step via elimination of HCl affording complex **3**. In the optimized structure of intermediate **B**, the distance between the metal-bound hydride and the closest methylene-hydrogen is found to be 1.080 Å subtending a C–H···H angle of 174.54°, indicating effective C–H···H hydrogen bonding interaction (*Fig.* S2). The rotational flexibility in the 2′,6′-diethylphenyl fragment and the resulting proximity between the methylene C–H and Ir–H bonds lead to cyclometalation via elimination of molecular hydrogen [65] yielding complex **4**. Isolation of the possible intermediates **A** and **B** has not been possible, probably due to their rapid transformation into the cyclometalated species **3** and **4**.

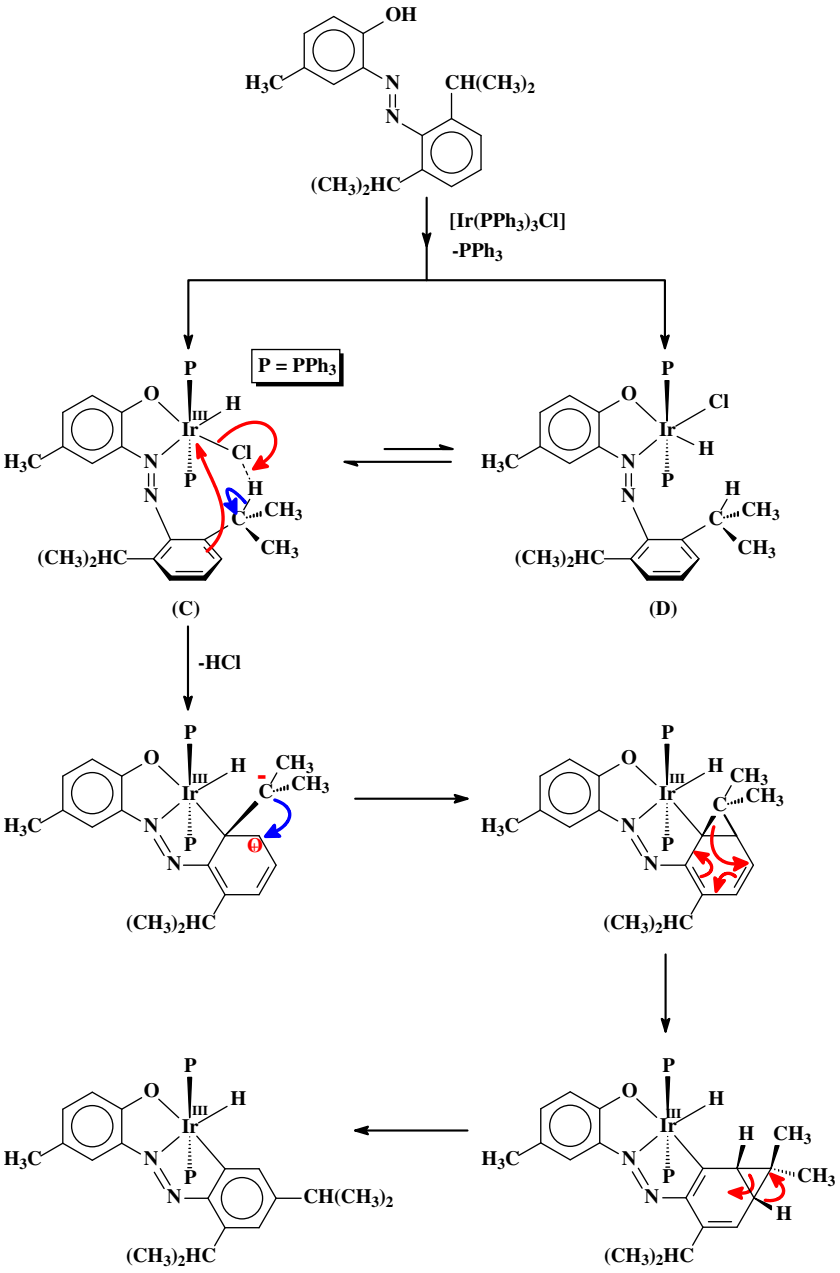

Scheme 2. Proposed steps for the formation of complex **5**.

During the formation of complex **5** (Scheme 2), ligand $\mathbf{L^3}$ is assumed to react initially with $[Ir(PPh_3)_3Cl]$ as before, generating two geometric isomers (**C** and **D**) of a hydride intermediate. Structures of both the intermediates have been geometrically optimized through DFT calculations and the optimized structures along with their respective energies are shown in *Fig.* S3 (Supplementary material). The intermediate **C** has significantly lower energy than intermediate **D**, indicating that the speculated equilibrium between these two species favors intermediate **C**. In the optimized structure of intermediate **C**, the central hydrogen of one *iso*-propyl group is involved in C–H···Cl hydrogen-bonding interaction with the metal-bound chloride (Cl···H distance = 1.527 Å, C–H···Cl angle = 105.59°). However, in the optimized structure of intermediate **D**, the Scheme 2 metal-bound hydride is 1.487 Å away from the central hydrogen of the proximal *iso*-propyl group, subtending a C–H···H angle of 104.76°, indicating a poorer hydrogen bonding interaction compared to that existing in the similar intermediate **B** in Scheme 1. Rapid elimination of HCl is believed to take place from intermediate **C**, leading to formation of a metal–carbon bond from an *ortho*-position (say, the 2′ position) of the phenyl ring in the phenylazo fragment, with consequent loss of aromaticity in that ring and the generation of a formal positive charge at the 3′ position. This fast reaction of **C** shifts the equilibrium between **C** and **D** more towards intermediate **C**. Elimination of HCl is also associated with generation of a carbanion at the central carbon of the de-protonated *iso*-propyl group, which then forms a C–C bond with the ring carbon at the 3′ position carrying the positive charge. This is followed by migration of the $C(CH_3)_2$ fragment, which was bound in an η^2-fashion to the 2′,3′ ring carbons, to the corresponding 3′,4′ position. In the next step usual rearrangements in the η^2-bound $C(CH_3)_2$ fragment take place, whereby the lost aromaticity of the aryl ring is restored and complex **5** is obtained.

Table 3
Electronic spectral and cyclic voltammetric data of the complexes.

Complex	Electronic spectral data[a] λ_{max}/nm (ε/M^{-1} cm^{-1})	Cyclic voltammetric data[b] E/V vs SCE
Complex **3**	544(2600), 382[c](2900), 306[c](7800), 272[c](11700)	1.10[d], 1.33[d], −0.96[e]
Complex **4**	537(2400), 388[c](3200), 324[c](7300), 276[c](12800)	1.03[d], 1.27[d], −1.07[e]
Complex **5**	636(6300), 394[c](6500), 348[c](9600), 256[c](37100)	0.66[d], 1.15[d], −1.03[e]

[a] In acetonitrile solution.
[b] Solvent, 1:9 dichloromethane–acetonitrile; supporting electrolyte, TBAP; scan rate 50 mV s^{-1}; reference electrode, SCE.
[c] Shoulder.
[d] Anodic peak potential (E_{pa}) value.
[e] Cathodic peak potential (E_{pc}) value.

Table 4
Composition of selected molecular orbitals.

Complex	Contributing fragments	% Contribution of fragments to	
		HOMO	LUMO
Complex **3**	Ir	1.14	1.19
	Triphenylphosphine	0.09	0.09
	Azo-ligand	98.77	98.72
Complex **4**	Ir	2.67	2.96
	Triphenyl phosphine	0	0.1
	Azo-ligand	97.039	96.85
Complex **5**	Ir	78.1	10.78
	Triphenyl phosphine	3.27	5.39
	Azo-ligand	18.53	83.63

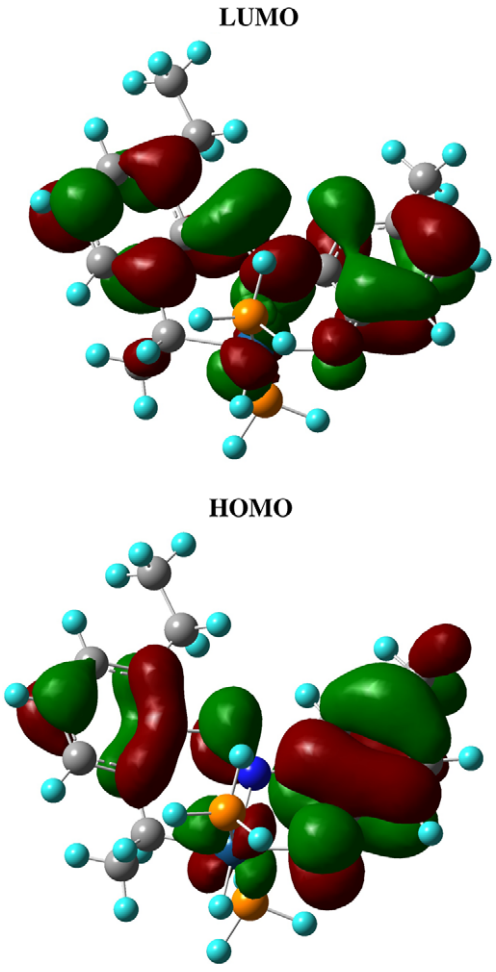

Fig. 3. Partial molecular orbital diagram of complex **3**.

2.2. Spectral studies

Magnetic susceptibility measurements show that complexes **3**, **4** and **5** are diamagnetic, consistent with the +3 oxidation state of iridium (low-spin d^6, $S = 0$) in these complexes. The ^1H NMR spectrum of each complex, recorded in $CDCl_3$ solution, shows broad signals in the range 7.04–7.48 ppm for the coordinated PPh_3 ligands. The methyl signal from the phenol fragment is observed as a distinct peak near 2.3 ppm. Signals from the ethyl and metal-bound $CHCH_3$ fragment in complexes **3** and **4**, as well as from *iso*-propyl groups in complex **5**, appear in the expected regions. Among the expected aromatic proton signals for the coordinated azo-ligands, most were clearly observed while a few could not be detected due to their overlap with the PPh_3 signals. Infrared spectra of complexes **3**, **4** and **5** show many bands of different intensities in the 400–4000 cm^{-1} region. Attempt to assign each band to a specific vibration has not been made. However, sharp bands displayed near 746, 694 and 520 cm^{-1} by all the three complexes are attributable to the coordinated PPh_3 ligands. Strong bands are also observed near 1483, 1434, 1245, 1188 and 1095 cm^{-1} in all these complexes, which are absent in the infrared spectrum of $[Ir(PPh_3)_3Cl]$, and hence these are assignable to the coordinated azo-ligands. The ^1H NMR and IR spectral data of the complexes are therefore consistent with their compositions.

The complexes **3**, **4** and **5** are found to be soluble in dichloromethane, chloroform, acetonitrile, acetone, etc., producing intense pink, red and blue solutions, respectively. Electronic spectra of these complexes have been recorded in acetonitrile solution. Each complex shows an intense absorption in the visible region and a few very strong absorptions in the ultraviolet region (Table 3). The absorptions in the ultraviolet region are assignable to transitions within the ligand orbitals. To understand the origin of the absorption in the visible region, electronic structures of the complexes have been probed with the help of DFT calculations [63,64] and the composition of selected molecular orbitals is given in Table 4. Electron distributions in the highest occupied molecular orbital (HOMO) and lowest unoccupied molecular orbital (LUMO) for complex **3** are shown in Fig. 3 and the same for complexes **4** and **5** are shown in *Figs. S4 and S5 (Supplementary material)*. In complexes **3** and **4**, both the HOMO and LUMO are distributed almost entirely over the azo-ligand. Hence the absorption in the visible region (near 540 nm) is assignable to a transition within the filled (HOMO) and vacant (LUMO) orbitals of the azo-ligand. In complex **5**, however, the HOMO is mostly (>78%) concentrated on the metal center, while the LUMO is primarily (>83%) delocalized over the coordinated azo-ligand. Hence the absorption at 636 nm is assignable to charge-transfer transition from iridium to the azo-ligand. It is interesting to note, particularly between the two hydride complexes **3** and **5**, that the nature of the HOMO depends on whether metallation occurs at an alkyl carbon (as in **3**) or at a phenyl carbon (as in **5**).

2.3. Electrochemical properties

Electrochemical properties of the complexes have been studied by cyclic voltammetry in 1:9 dichloromethane–acetonitrile solution (0.1 M TBAP) [66]. Voltammetric data are given in Table 3. Complexes **3** and **4** show two oxidative responses on the positive side of SCE and a reductive response on the negative side. In view of the composition of the HOMO in these two complexes, the first oxidative response is assigned to oxidation of the coordinated azo-ligand. Similarly based on the composition of the LUMO, the reductive response is assigned to reduction of the coordinated azo-ligand. The second oxidative response is tentatively assigned to oxidation of the coordinated azo-ligand. Complex **5** also shows two oxidative responses on the positive side of SCE and a reductive response on the negative side. However, as the HOMO in this complex is largely an iridium-based orbital, the first oxidative response is assigned to Ir(III)–Ir(IV) oxidation. The other two redox responses are assigned, as before, to oxidation and reduction of the coordinated azo-ligand. All the redox responses for all three complexes are irreversible.

3. Conclusions

Along with our earlier observations [52], the present study shows that blocking both the 2′,6′ positions of the 2-(arylazo)phenol (**I**) by alkyl groups can successfully induce metal-mediated C–H or C–C bond activation of one alkyl (R) group at one of these two positions. This has been manifested in the reaction of 2-(2′,6′-dialkylphenylazo)-4-methylphenols (**III**) with $[Ir(PPh_3)_3Cl]$. In the case of R = methyl and ethyl, C–H activation of the alkyl group takes place, whereas when R = *iso*-propyl, migration of an *iso*-propyl group occurs via C–C activation. These studies thus demonstrate that the nature of bond activation of the alkyl group in ligands of type III and the organoiridium complexes produced from these depend primarily on the size of the alkyl group attached to the alpha-carbon.

4. Experimental

Iridium trichloride was obtained from Arora Matthey, Kolkata, India. All other chemicals and solvents were reagent grade commercial materials and were used as received. $[Ir(PPh_3)_3Cl]$ was synthesized by following a reported procedure [46]. The 2-(2′,6′-diethylphenylazo)-4-methylphenol and 2-(2′,6′-diisopropylphenylazo)-4-methylphenol were prepared following reported procedures [53]. Purification of dichloromethane and acetonitrile, and preparation of tetrabutylammonium perchlorate (TBAP) for electrochemical work were performed following reported procedures [67,68]. Microanalyses (C, H, N) were performed using a Heraeus Carlo Erba 1108 elemental analyzer. Mass spectra were recorded with a Micromass LCT electrospray (Qtof Micro YA263) mass spectrometer by electrospray ionization method. IR spectra were obtained on a Shimadzu FTIR-8300 spectrometer with samples prepared as KBr pellets. Electronic spectra were recorded on a JASCO V-570 spectrophotometer. Magnetic susceptibilities were measured using a PAR 155 vibrating sample magnetometer fitted with a Walker scientific L75FBAL magnet. ^{1}H NMR spectra were recorded in $CDCl_3$ solution on a Bruker Avance DPX 300 NMR spectrometer using TMS as the internal standard. Electrochemical measurements were made using a CH Instruments model 600A electrochemical analyzer. A platinum disc working electrode, a platinum wire auxiliary electrode and an aqueous saturated calomel reference electrode (SCE) were used in a three-electrode configuration. All electrochemical experiments were performed under a dinitrogen atmosphere. All electrochemical data were collected at 298 K and are uncorrected for junction potentials. Optimization of ground-state structures and energy calculations of the organoiridium complexes were carried out by density functional theory (DFT) method using the GAUSSIAN 03 (B3LYP/SDD-6-31G) package [63].

4.1. Synthesis of complexes

Complexes **3** and **4**. A solution of 2-(2′,6′-diethylphenylazo)-4-methylphenol (26 mg, 0.10 mmol) in toluene (40 mL) was purged with a stream dinitrogen for 5 min. To this solution were added triethylamine (10 mg, 0.10 mmol) and $[Ir(PPh_3)_3Cl]$ (100 mg, 0.10 mmol) successively. The resulting mixture was then heated at reflux under a dinitrogen atmosphere for 24 h to yield an orange solution. The solvent was then evaporated to give a solid mass, which was subjected to purification by thin layer chromatography on a silica plate. With benzene as the eluant, a pink band followed by a red band separated, and these were extracted with acetonitrile. Concentration of these extracts gave complexes **3** and **4** as crystalline pink and red solids, respectively. Complex **3**: Yield: 22%. *Anal.* Calc. for $C_{53}H_{49}N_2OP_2Ir$: C, 64.69; H, 4.98; N, 2.85. Found: C, 64.54; H, 4.78; N, 2.78%. Mass: 983, $[M-H]^+$; 955, $[M-(H+C_2H_4)]^+$. ^{1}H NMR [69]: −21.34 (t, hydride, J = 12.6); 1.26 (t, 3H, J = 7.5); 1.75 (d, 3H, J = 4.2); 2.40 (CH_3); 2.74 (q, 2H, J = 7.5); 3.52 (q, 1H, J = 7.2); 7.10–7.34*(2H+2PPh$_3$); 7.46 (t, 1H, J = 7.2); 7.64 (d, 1H, J = 8.2); 7.66 (d, 1H, J = 8.3). Complex **4**: Yield: 30%. *Anal.* Calc. for $C_{53}H_{48}N_2OP_2ClIr$: C, 62.49; H, 4.72; N, 2.75. Found: C, 62.14; H, 4.63; N, 2.63%. Mass: 983, $[M-Cl]^+$; 955, $[M-(Cl+C_2H_4)]^+$. ^{1}H NMR: 1.20 (t, 3H, J = 7.5); 1.98 (d, 3H, J = 4.2); 2.39 (CH_3); 2.71 (q, 2H, J = 7.5); 4.19 (q, 1H, J = 7.0); 6.96 (d, 1H, J = 8.4); 7.04–7.46*(1H+2PPh$_3$); 7.49 (t, 1H, J = 7.1); 7.55 (d, 1H, J = 6.3); 7.63 (d, 1H, J = 6.3).

Complex **5**. This complex was prepared by following the same procedure as above but using 2-(2′,6′-diisopropylphenylazo)-4-methylphenol instead of 2-(2′,6′-diethylphenylazo)-4-methylphenol. Complex **5** was obtained as a crystalline blue solid. Yield: 40%. *Anal.* Calc. for $C_{55}H_{53}N_2OP_2Ir$: C, 65.27; H, 5.24; N, 2.77. Found: C, 65.35; H, 5.26; N, 2.73%. Mass: 1011, $[M-H]^+$. ^{1}H NMR: −17.06 (t, hydride, J = 15.3); 0.68 (d, 6H, J = 6.6); 0.76 (d, 6H, J = 6.8); 2.21 (CH_3); 3.26 (m, 1H, J = 6.9); 3.41 (m, 1H, J = 7.2); 6.01 (s, 1H); 6.38 (s, 1H); 6.66 (s, 1H); 6.47 (d, 1H, J = 8.6); 6.94 (d, 1H, J = 8.6); 7.05–7.48*(2PPh$_3$).

4.2. X-ray structure determination

Single crystals of complex **5** were grown by slow evaporation of the solvent from an acetonitrile solution of the complex. Selected

Table 5
Crystallographic data for complex **5**.

Empirical formula	$C_{55}H_{53}N_2OP_2Ir$
Formula weight	1012.14
Space group	Triclinic, P1
a (Å)	12.0985(8)
b (Å)	13.7457(9)
c (Å)	14.8119(10)
α (°)	86.583(2)
β (°)	67.888(2)
γ (°)	82.637(2)
V (Å^3)	2263.1(3)
Z	2
λ (Å)	0.71073
Crystal size (mm)	0.11 × 0.19 × 0.20
T (K)	150
μ (mm^{-1})	3.063
R_1[a]	0.0285
wR_2[b]	0.0642
Goodness-of-fit (GOF)[c]	1.03

[a] $R_1 = \Sigma||F_o| - |F_c||/\Sigma|F_o|$.
[b] $wR_2 = [\Sigma[w(F_o^2 - F_c^2)^2]/\Sigma[w(F_o^2)^2]]^{1/2}$.
[c] GOF = $[\Sigma[w(F_o^2 - F_c^2)^2]/(M - N)]^{1/2}$, where M is the number of reflections and N is the number of parameters refined.

crystal data and data collection parameters are given in Table 5. Data were collected on a Bruker SMART1000 CCD diffractometer using graphite monochromated Mo Kα radiation. Structure solution by direct methods and refinement by least squares were carried out using the SHELXS97 and SHELXL97 programs, respectively [70].

Acknowledgements

The authors thank the reviewers for their constructive comments, which have been helpful in preparing the revised manuscript. Financial assistance received from the Department of Science and Technology, New Delhi [Grant No. SR/S1/IC-15/2004] is gratefully acknowledged. Dipravath Kumar Seth thanks the Council of Scientific and Industrial Research, New Delhi, for his fellowship [Grant No. 9/096(0511)/2006-EMR I]. HT and AJB thank the EPSRC (UK) for the award of a single-crystal X-ray diffractometer.

Appendix A. Supplementary material

CCDC 706553 contains the supplementary crystallographic data for this paper. These data can be obtained free of charge from The Cambridge Crystallographic Data Centre via www.ccdc.cam.ac.uk/data_request/cif. Supplementary data associated with this article can be found, in the online version, at doi:10.1016/j.jorganchem.2010.01.015.

References

[1] B.M. Trost, T.R. Verhoeven, Comprehensive Organometallic Chemistry, in: E. Abel, F.G.A. Stone, G. Wilkinson (Eds.), Pergamon Press, Oxford, 1982, p. 8.
[2] J.P. Collman, L.S. Hegedus, J.R. Norton, R.G. Finke, Principles and Applications of Organotransition Metal Chemistry, Mill Valley, CA, 1987.
[3] L.S. Hegedus, Transition Metals in the Synthesis of Complex Organic Molecules, Mill Valley, CA, 1994.
[4] E. Abel, F.G.A. Stone, G. Wilkinson (Eds.), Comprehensive Organometallic Chemistry, Pergamon Press, Oxford, 1995, p. 12.
[5] L.S. Liebeskind (Ed.), Advances in Metal-Organic Chemistry, Jai Press, Greenwich, CT, 1996.
[6] B. Cornils, W.A. Hermann (Eds.), Applied Homogenous Catalysis with Organometallic Compounds: A Comprehensive Handbook in Two Volumes, VCH, Weinheim, 1996.
[7] M. Bellar, C. Bolm (Eds.), Transition Metals for Organic Synthesis **1–2**, Wiley-VCH, Weinheim, 1998.
[8] L.S. Hegedus, Coord. Chem. Rev. 168 (1998) 49.
[9] J. Tsuji, Transition Metal Reagents Catalysts, Wiley-VCH, Weinheim, 2000.
[10] A. de Meijere, Chem. Rev. 100 (2000) 2739.
[11] F. Alonso, I.P. Beletskaya, M. Yus, Chem. Rev. 102 (2002) 4009.
[12] C.M. Che, J.S. Huang, Coord. Chem. Rev. 242 (2003) 97.
[13] B.M. Trost, M.L. Crawley, Chem. Rev. 103 (2003) 2921.
[14] T. Mallat, A. Baiker, Chem. Rev. 104 (2004) 3037.
[15] B.H. Lipshutz, Y. Yamamoto, Chem. Rev. 108 (2008) 2793.
[16] N.A. Foley, J.P. Lee, Z. Ke, T.B. Gunnoe, T.R. Cundari, Acc. Chem. Res. 42 (2009) 585.
[17] C. Jia, T. Kitamura, Y. Fujiwara, Acc. Chem. Res. 34 (2001) 633.
[18] C. Slugovc, I. Padilla-Martnez, S. Sirol, E. Carmona, Coord. Chem. Rev. 213 (2001) 129.
[19] A. Vigalok, D. Milstein, Acc. Chem. Res. 34 (2001) 798.
[20] K. Matsumoto, M. Ochiai, Coord. Chem. Rev. 231 (2002) 229.
[21] V. Ritleng, C. Sirlin, M. Pfeffer, Chem. Rev. 102 (2002) 1731.
[22] C.S. Chin, G. Won, D. Chong, M. Kim, H. Lee, Acc. Chem. Res. 35 (2002) 218.
[23] K. Matsumoto, H. Sugiyama, Acc. Chem. Res. 35 (2002) 915.
[24] C.B. Pamplin, P. Legzdins, Acc. Chem. Res. 36 (2003) 223.
[25] M.E.V. Boom, D. Milstein, Chem. Rev. 103 (2003) 1759.
[26] H.-Y. Jang, M.J. Krische, Acc. Chem. Res. 37 (2004) 653.
[27] S.R. Klei, K.L. Tan, J.T. Golden, C.M. Yung, R.K. Thalji, K.A. Ahrendt, J.A. Ellman, T.D. Tilley, R.G. Bergman, Activation and Functionalization of C–H Bonds, 2004, pp. 46–55 (Chapter 2).
[28] P. Legzdins, C.B. Pamplin, Activation and Functionalization of C–H Bonds, 2004, pp. 184–197 (Chapter 11).
[29] H.A.Y. Mohammad, J.C. Grimm, K. Eichele, H.G. Mack, B. Speiser, F. Novak, W.C. Kaska, H.A. Mayer, Activation and Functionalization of C–H Bonds, 2004, pp. 234–247 (Chapter 14).
[30] E. Carmona, M. Paneque, L.L. Santos, V. Salazar, Coord. Chem. Rev. 249 (2005) 1729.
[31] M. Lersch, M. Tilset, Chem. Rev. 105 (2005) 2471.
[32] W. Leis, H.A. Mayer, W.C. Kaska, Coord. Chem. Rev. 252 (2008) 1787.
[33] Y.J. Park, J.W. Park, C.H. Jun, Acc. Chem. Res. 41 (2008) 222.
[34] J.C. Lewis, R.G. Bergman, J.A. Ellman, Acc. Chem. Res. 41 (2008) 1013.
[35] O. Daugulis, H.Q. Do, D. Shabashov, Acc. Chem. Res. 42 (2009) 1074.
[36] F. Basuli, S.M. Peng, S. Bhattacharya, Inorg. Chem. 40 (2001) 1126.
[37] I. Pal, S. Dutta, F. Basuli, S. Goverdhan, S.M. Peng, G.H. Lee, S. Bhattacharya, Inorg. Chem. 42 (2003) 4338.
[38] P. Gupta, R.J. Butcher, S. Bhattacharya, Inorg. Chem. 42 (2003) 5405.
[39] R. Acharyya, S. Dutta, F. Basuli, S.-M. Peng, G.-H. Lee, L.R. Falvello, S. Bhattacharya, Inorg. Chem. 45 (2006) 1252.
[40] S. Basu, S. Dutta, M.G.B. Drew, S. Bhattacharya, J. Organomet. Chem. 691 (2006) 3581.
[41] S. Baksi, R. Acharyya, S. Dutta, A.J. Blake, M.G.B. Drew, S. Bhattacharya, J. Organomet. Chem. 692 (2007) 1025.
[42] S. Nag, R.J. Butcher, S. Bhattacharya, Eur. J. Inorg. Chem. (2007) 1251.
[43] C. GuhaRoy, S.S. Sen, S. Dutta, G. Mostafa, S. Bhattacharya, Polyhedron 26 (2007) 3876.
[44] S. Dutta, S.M. Peng, S. Bhattacharya, J. Chem. Soc., Dalton Trans. (2000) 4623.
[45] K. Majumder, S.M. Peng, S. Bhattacharya, J. Chem. Soc., Dalton Trans. (2001) 284.
[46] R. Acharyya, F. Basuli, R.-Z. Wang, T.C.W. Mak, S. Bhattacharya, Inorg. Chem. 43 (2004) 704.
[47] P. Gupta, S. Dutta, F. Basuli, S.-M. Peng, G.-H. Lee, S. Bhattacharya, Inorg. Chem. 45 (2006) 460.
[48] S. Halder, R. Acharyya, S.M. Peng, G.H. Lee, M.G.B. Drew, S. Bhattacharya, Inorg. Chem. 45 (2006) 9654.
[49] S. Halder, M.G.B. Drew, S. Bhattacharya, Organometallics 25 (2006) 5969.
[50] R. Acharyya, S.M. Peng, G.H. Lee, S. Bhattacharya, Inorg. Chem. 42 (2003) 7378.
[51] S. Nag, P. Gupta, R.J. Butcher, S. Bhattacharya, Inorg. Chem. 43 (2004) 4814.
[52] R. Acharyya, F. Basuli, S.M. Peng, G.H. Lee, R.Z. Wang, T.C.W. Mak, S. Bhattacharya, J. Organomet. Chem. 690 (2005) 3908.
[53] S. Baksi, R. Acharyya, F. Basuli, S.M. Peng, G.H. Lee, M. Nethaji, S. Bhattacharya, Organometallics 26 (2007) 6596.
[54] M. Akhter, K.A. Azam, S.M. Azad, S.E. Kabir, K.M. Abdul Malik, R. Mann, Polyhedron 22 (2003) 355.
[55] S.P. Tunik, I.A. Balova, M.E. Borovitov, E. Norlander, M. Haukka, T.A. Pakknen, J. Chem. Soc., Dalton Trans. (2002) 827.
[56] R.L. Zuckerman, S.W. Krska, R.G. Bergman, J. Organomet. Chem. 608 (2000) 172.
[57] A. Zucca, M.A. Cinellu, M.V. Pinna, S. Stoccoro, G. Minghetti, M. Manassero, M. Sansoni, Organometallics 19 (2000) 4295.
[58] J.A.M. Brandts, E. Kruiswijk, J. Boersma, A.L. Spek, G. Van Koten, J. Organomet. Chem. 585 (1999) 93.
[59] J.R. Torkelson, R. McDonald, M. Cowie, Organometallics 18 (1999) 4134.
[60] P.J. Alaimo, R.G. Bergman, Organometallics 18 (1999) 2707.
[61] H.F. Luecke, R.G. Bergman, J. Am. Chem. Soc. 119 (1997) 11538.
[62] H.F. Luecke, B.A. Arndtsen, P. Burger, R.G. Bergman, J. Am. Chem. Soc. 118 (1996) 2517.
[63] M.J. Frisch, G.W. Tracks, H.B. Schlegel, G.E. Scuseria, M.A. Robb, J.R. Cheeseman Jr., J.A. Montgomery, T. Vreven, K.N. Kudin, J.C. Burant, J.M. Millam, S.S. Iyengar, J. Tomasi, V. Barone, B. Mennucci, M. Cossi, G. Scalamani, N. Rega, G.A. Petersson, H. Nakatsuji, M. Hada, M. Ehara, K. Toyota, R. Fukuda, I. Hasegawa, M. Ishida, T. Nakajima, Y. Honda, O. Kitao, H. Nakai, M. Klene, X. Li, J.E. Knox, H.P. Hratchian, J.B. Cross, V. Bakken, C. Adamo, J. Jaramillo, R. Gomperts, R.E. Stratmann, O. Yazyev, A.J. Austin, R. Cammi, C. Pomelli, J.W. Ochterski, P.Y. Ayala, K. Morokuma, G.A. Voth, P. Salvador, J.J. Dannenberg, V.G. Zakrzewski, S. Dapprich, A.D. Daniels, M.C. Strain, O. Farkas, D.K. Malick, A.D. Rabuck, K. Raghavachari, J.B. Foresman, J.V. Ortiz, Q. Cui, A.G. baboul, S. Clifford, J. Cioslowski, B.B. Stefanov, G. Liu, A. Liashenko, P. Piskroz, I. Komaromi, R.L. Martin, D.J. Fox, T. Keith, M.A. Al-Laham, C.Y. Peng, A. Nanayakkara, M. Challacombe, P.M.W. Gill, B. Johnson, W. Chen, M.W. Wong, C. Gonzalez, J.A. Pople, Gaussian 03, revision D01, Gaussian Inc., Pittsburgh, PA, 2003.
[64] In optimizing the structures of complexes **3** and **4**, the crystal structure of complex **1** has been used as the starting model and necessary modifications have been made. Phenyl rings of the PPh_3 ligands have been replaced by hydrogens.
[65] The evolved hydrogen could not be detected.
[66] A little dichloromethane was necessary to take the complex into solution. Addition of a large excess of acetonitrile was necessary to record the redox responses in proper shape.
[67] D.T. Sawyer, J.L. Roberts Jr., Experimental Electrochemistry for Chemists, Wiley, New York, 1974.
[68] M. Walter, L. Ramaley, Anal. Chem. 45 (1973) 165.
[69] Chemical shifts are given in ppm and multiplicity of the signals along with the associated coupling constants (*J* in Hz) are given in parentheses. Overlapping signals are marked with an asterisk.
[70] G.M. Sheldrick, Acta Crystallogr., Sect. A 64 (2008) 112.